The Standard Capacity Model: Towards a Polyhedron Representation of Container Vessel Capacity*

Rune Møller Jensen[1] and Mai Lise Ajspur[1]

IT University, Rued Langaards Vej 7, 2300 Copeenhagen S, Denmark

Abstract. Container liner shipping is about matching spare capacity to cargo in need of transport. This can be realized using cargo flow networks, where edges are associated with vessel capacity. It is hard, though, to calculate free capacity of container vessels unless full-blown non-linear stowage optimization models are applied. This may cause such flow network optimization to be intractable. To address this challenge, we introduce the Standard Capacity Model (SCM). SCMs are succinct linear capacity models derived from vessel data that can be integrated in higher order optimization models as mentioned above. In this paper, we introduce the hydrostatic core of the SCM. Our results show that it can predict key parameters like draft, trim, and stress forces accurately and thus can model capacity reductions due to these factors.

Keywords: Container vessel capacity · Stowage planning · Linear modelling.

1 Introduction

Container liner shipping is a major driver of the world economy [4]. Today, there are more than 5000 container vessels in the world [14], mostly sailing on cyclic services with published fixed weekly schedules and freight rates. Liner shipping companies adjust these service networks and their fleet over the year to fit seasonal trends and long-term developments in the world economy, but they seldom make fleet and network changes due to current cargo on the network and known bookings. For that reason, it is a central objective to maximize the utilization of the service network, as any free capacity in the network is a business opportunity.

Previous work has studied how to apply revenue management methods in the liner shipping industry similar to the ones successfully applied in the airline industry (e.g., [16]). This has turned out to be challenging in practice. A major obstacle is to compute the free capacity of a container vessel. Although surprising at first, it is not simply the number of vacant slots on the vessel, since a large number of local and global constraints may cause slots to be impossible to use. These constraints include: stacking limitations due to different length, height,

* This research is supported by the Danish Maritime Fund, Grant No. 2016-064.

power need (reefer containers), and dangerous content of containers; limited volume, weight, and securing capacity of container stacks; vessel hydrostatics like stability requirements and stress force limitations; containers blocking each other due to different port of discharge; capacity preserving stowage patterns; and work balancing of quay cranes. It is recognized by leading economists that this problem blocks a paradigm change in liner shipping. According to Stopford, the ability to match spare capacity to cargo in need of transportation on the fly would allow the "Uberisation" of the freight business [5]. Today, the higher sales and cargo flow functions in liner shipping companies are unable to make these matchings. The spare capacity of a container vessel is often simply calculated as its maximum volume, weight, and reefer container capacity subtracted the capacity taken up by on board cargo without consideration of losses due stowage restrictions and rules. This can cause great over-estimates of the free capacity of the vessels [3].

In the last two decades, a number of automated stowage planning methods have been published (e.g.,[15, 7, 8, 10, 1, 12]). The input to these methods is the arrival condition of the vessel and a list of containers to load, and the output is a stowage plan. As such, these methods are unable to compute the spare capacity of the vessel, since the containers to load are assumed to be known. Several of the contributions, though, apply optimization models, where the containers to load can act as decision variables rather than constants (e.g., [1, 3, 10]). These models can be used to compute the spare capacity of a vessel. In practice, though, they can be challenging to apply in higher functions such as sales and cargo flow. The stowage planning problem is NP-hard [2], even in its various abstract versions [13]. This means that the stowage optimization models can take long time to solve, which also happens in practice (e.g., [10]). Since it can take more than five hours to generate a stowage plan manually, this is an acceptable evil in stowage planning. In higher functions, on the other hand, capacity models can be parts of larger optimization models which require that they are scalable. For instance, in capacity and uptake management, a cargo flow network could be used to match cargo demand with spare capacity. In such a network modelling several weeks of a major trade line, there are thousands of edges representing voyage legs, and each of these needs to be associated with a capacity model.

To address this challenge, this paper introduces the *Standard Capacity Model* (SCM). The SCM is based on several insights from previous work on stowage planning optimization. First, a significant source of the complexity and inaccessibility of these models is the spatial misalignment of data describing container vessels. To clear this, the SCM interpolates vessel data to align with the endpoints of each bay. Second, stowage optimization models have many details that can be abstracted away in capacity calculations. To this end, the granularity of the SCM can be adjusted. At the finest level, each bay forms a *section*. At coarser levels, adjacent sections are merged. Third, a previous study of vessel hydrostatics show that these can be accurately approximated by linear functions for a fixed displacement [11]. Container vessels at normal drafts, however, are near

box-formed. This opens for a linear formulation of the hydrostatic equilibrium equations at any displacement that until now has not been exploited.

The intractable elements of stowage planning include separation rules of containers with dangerous goods and the fact that quay cranes only can discharge containers from the top of stacks [2]. In more abstract capacity models, though, it may be possible to express some of these combinatorial aspects as linear trade-offs. In particular, a significant body of industrial work shows that surprisingly many highly complex aspects of stowage planning can be linearly expressed [9]. Our objective is in time to mature the SCM with these advanced linear models. In this paper, we focus on the hydrostatic core of the SCM that to our knowledge is the first linear approximation of the hydrostatic equilibrium of a container vessel for variable displacement. Our results show that the hydrostatic model is able to predict key parameters like draft, trim, and stress forces with a sufficient accuracy for practical application even for coarse standard capacity models.

The remainder of this paper is organized as follows. We define the problem in Section 2 and introduce the SCM in Section 3. In Section 4, we evaluate the prediction accuracy of the SCM, and finally in Section 5 we conclude and discuss directions of future work.

2 Problem Formulation

Container vessels mainly transport ISO containers with the dominating lengths 20', 40', and 45', while the containers usually are 8' wide. There are two common heights: standard 8'6" (DC) and high-cube 9'6" (HC). Containers have corner fittings that allow them to be stacked about 10 high. 45DC and 20HC are rare. *Reefer* containers are refrigerated and need external power. *Out-of-gauge* (OOG) containers have irregular dimensions (e.g., open top containers with cargo sticking up). Flatracks are flat containers to carry non-containerized cargo (break-bulk). *DG* containers contain dangerous goods such as fireworks and chemicals. They must be placed according to complex separation rules and may not be allowed near reefers since these are spark generators.

As shown in Fig. 1, the cargo space of a container vessel is divided into *bays*, which each consists of stacks (rows) of cells. A cell is divided into a fore and aft *slot* and can accordingly hold one 40' (or 45') container or two 20' containers. Some cells have power plugs allowing reefers to be stowed. Each bay is divided into stowage areas above and under *hatch covers* that separate on deck and below deck cells. A vessel has a cargo securing manual that details how the vessel can be stowed securely. The precise position of bays, fuel tanks and ballast water tanks are provided by the shipyard that build the vessel. The yard also provides details about the *lightship*, which is the vessel without cargo, fuel or ballast water. This information can be given as a set of blocks with known mass and center of gravity as shown in Fig. 1. From this data, the resulting center of gravity of the vessel can be calculated.

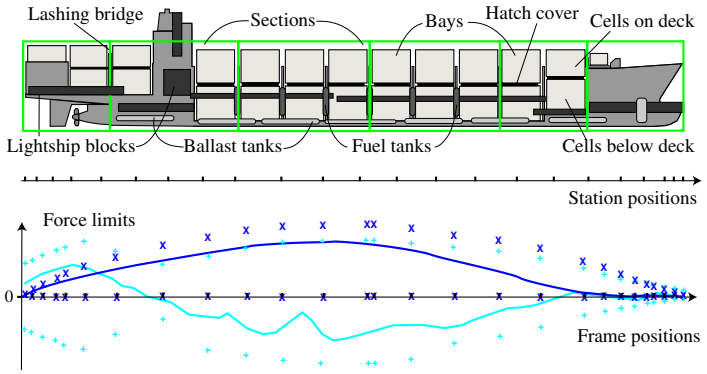

Fig. 1. Top: the structure of a cellular container vessel and an example of a section partitioning that can be used by the SCM. Bottom: an example of the shear forces (light blue curve) and bending moments (dark blue curve) along a vessel. Light blue plus signs and dark blue crosses are the associated force limits given by the classification society for a set of frame positions.

The Bonjean table of the vessel can be used to compute its center of buoyancy. For a set of cross-sections called *stations* along the vessel, the table gives the submerged area as a function of the distance from the keel to the water line (*draft*) of the station. A vessel is in hydrostatic equilibrium when the center of buoyancy and gravity are vertically aligned. In this condition, the vessel floats at rest in the water at a stable draft and *trim*. Trim is the difference between aft and fore draft of the vessel (i.e., nose up is positive trim). The total weight of a vessel is referred to as its *displacement* and has different summer and winter limits depending on sea location. Many ports such as Hamburg have significant tide dependent draft limits. Fuel efficient trims are typically around -2 meters (i.e., nose down).

While the sum of buoyancy and gravity forces are vertically aligned at hydrostatic equilibrium, the forces acting on the vessel are usually distributed unevenly over the hull. Fig. 2 shows an example of the resulting gravity and

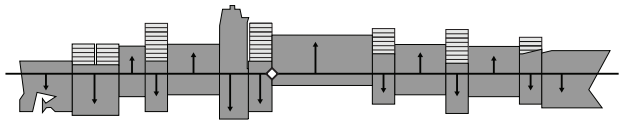

Fig. 2. An example of the resulting forces (black arrows) acting in the longitudinal direction at hydrostatic equilibrium.

buoyancy forces and how they would cause sections of the vessel to change draft if they could move freely. The counteracting forces in the hull that prevents such movement are referred to as *stress forces*. The critical stress forces acting on a

vessel are *shear forces* (SF), *bending moments* (BM), and *torsion moments* (TM). These forces are defined relative to a cross-section of the vessel. Consider the cross-section indicated by the white diamond in Fig. 2. SF at the cross-section is the sum of forces fore of the cross-section. [1] BM is the sum of forces each multiplied with the longitudinal distance to them. TM is caused by the distribution of forces over the center line. It is defined like BM using the transversal distance to the force. SF and BM measure how much the forces try to shear and bend the cross-section, while TM measures how much they try to twist it. The classification society of the vessel defines minimum and maximum limits of these forces for a number of frame positions along the vessel. Fig. 1 shows an example of SF and BM forces. Notice that frame and station positions are misaligned. A ship typically has higher gravity forces than buoyancy forces in the bow and stern. Consequently, SF forces are positive aft and negative fore, while BM is high midship.

3 The Standard Capacity Model

The purpose of the Standard Capacity Model (SCM) is to: 1) simplify the data representation of vessels by aligning all data points to a reference system defined by sections; 2) simplify the capacity constraints of vessels by a linear polyhedron approximation; and 3) provide a model with an adjustable level of detail. As mentioned in the introduction, the key idea of the SCM is to partition the vessel into sections that are aligned with bays. At the finest level of detail, sections hold at most one bay. At coarser levels, some sections are merged. As an example, Fig. 1 shows a partitioning of a vessel into six sections, where the largest sections aggregate three bays each. The choice of sections depends on the application. For large cargo flow models, it may only be computationally tractable with a few sections per vessel. The choice also depends on the cellular structure of the vessel. A section partitioning also should be made with stowage trade-offs in mind (e.g., cluster bays with same reefer plug and lashing bridge arrangement).

This paper focuses on the main building block of the SCM which, to our knowledge, is the first linear approximation to a hydrostatic model of a container vessel that allows variable displacement. We model the hydrostatic equilibrium of forces acting on the vessel in the longitudinal direction. This enables the SCM to model core parameters such as draft, trim, BM, and SF, and the approach is possible to extend in the transversal and vertical direction to model list, TM, and metacentric height. For this purpose, we need to approximate the relations between the variables of the SCM (see Table 1) as linear equations.

The mass of a section is the sum of masses of lightship blocks, ballast water, fuel, and cargo within the boundaries of the section. If a block (e.g., a ballast water tank) extends beyond the section, only the mass of the fraction within the section is included in the sum. If we assume that all gravity forces act from the

[1] SF can just as well be defined as the sum of forces aft of the cross-section. The reason is that since the vessel is at hydrostatic equilibrium, the two forces must be equal, but with opposite sign.

longitudinal mid-point of the section, the resulting gravity force clearly can be expressed as a linear function of the cargo and ballast water in the section. [2]

The buoyancy of a section depends on the draft of the section rather than its weight. It can be estimated from the Bonjean table of the vessel. Recall that the Bonjean table for each station gives the submerged area of a cross-section at the station as a function of the mid-ship draft at even keel. Fig. 3 shows the Bonjean data of a 15000 TEU container vessel with a representative fine form hull. Notice that the curves are shown over the complete operational draft range of the vessel. The lightship draft is about four meters and the maximum summer draft is about 16 meters.

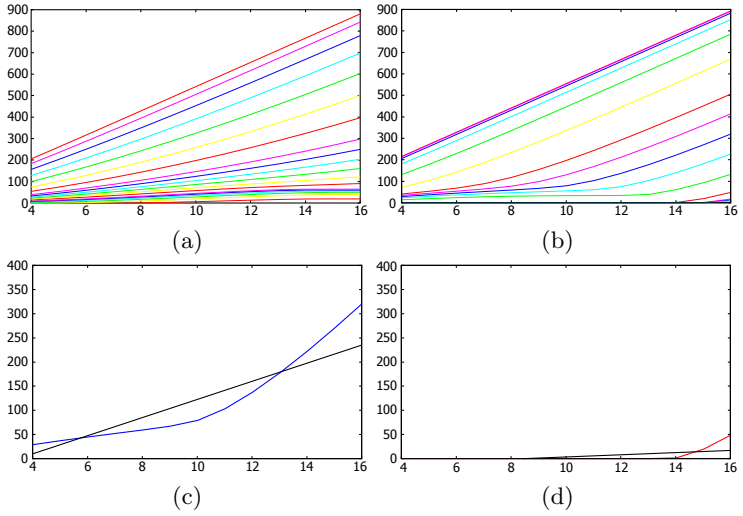

Fig. 3. Subermged area of fore (a) and aft (b) stations as a function of mid-ship draft at even keel. Two examples of linearisations of aft curves (c,d).

The mid-ship stations (top curves in graph (a) and (b)) have the largest submerged areas. Since the vessel has vertical sides at drafts above four meters in this part, the submerged areas grow linearly with the draft from this level. The curves for fore sections are slightly non-linear, while they are significantly non-linear for the aft sections (lower curves graph (b)). The reason is that the full stern only touches the water at maximum draft.

Despite these non-linearities, the dominating shape of the vessel is box-formed with vertical sides within the operational draft area. This means that the horizontal surface formed by the water line approximately has fixed shape such that the longitudinal moment needed to achieve a particular trim adjustment (say plus one meter) is constant for different displacements. This conclusion

[2] In future versions of the SCM, this point may be divided in the transversal and vertical direction to estimate TM and metacentric height.

seems in conflict with previously published data shown in Fig. 4(a). The graph shows trim as a function of displacement (i.e., draft) and longitudinal center of gravity (lcg) for the same vessel. For a fixed lcg (i.e., fixed longitudinal moment) this graph shows a highly non-linear relation between trim and displacement. A closer inspection of the graph, however, reveals that the displacement range is far out of operational levels which are above a fuelled ship of about 75K tons and below maximum summer displacement of 218K tons. Between 100K and 218K, we do see a rather linear relation between trim and displacement as expected from the analysis above. Due to this, we approximate the vessel as box-formed

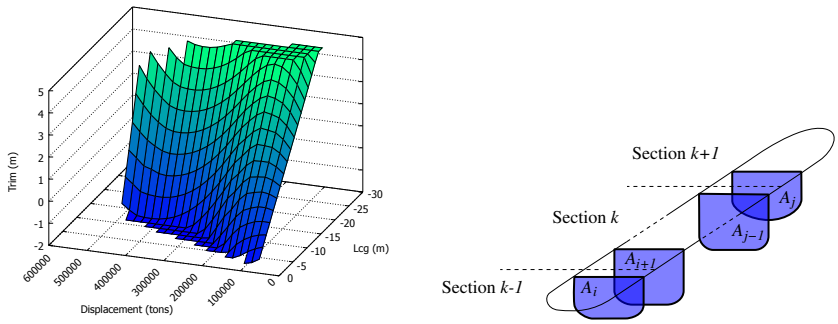

(a) (b)

Fig. 4. (a) Trim as a function of displacement and lcg [11]. (b) Bouyancy approximation of a section.

sections. To this end, the SCM uses a linear approximation to all Bonjean curves. Two examples of the linearisations of aft curves are shown in Fig. 3(c,d). Assume that the two boundaries of section k lie between station i and $i+1$ and $j-1$ and j, respectively, as shown in Fig. 4(b). Further assume that the submerged area of station v is A_v according to the linearisation above. We then have that the buoyancy of section k in tons is

$$\frac{d}{2}\sum_{v=i}^{j-1} f_v l_v (A_{v+1} + A_v), \tag{1}$$

where d is the density of salt water, f_v is the longitudinal fraction of station v to $v+1$ within the boundary of section k, and l_v is the distance between the two stations. At maximum summer displacement of the example vessel, this approximation underestimates the buoyancy with about 3.06%. This is probably due to the slightly convex shape of the hull. Consequently we adjust the linearisation such that it predicts the correct summer displacement.

Below we present the SCM as an LP feasible set (i.e., a polyhedron). Table 1 contains the explanation of symbols for sets, constants, and variables used in the model. Sections are numbered from the bow (i.e., $\mathcal{S} = \{1, 2, \ldots\}$). They form a

$\mathcal{S}$	Set of sections.
$\mathcal{T}$	Set of container types.
L_s	Length of section s in meters.
W_s^0	Lightship weight of section s in tons.
$\mathrm{SF}_s^{+/-}$	Positive and negative shear force limit in tons.
$\mathrm{BM}_s^{+/-}$	Positive and negative bending moment limit in tons meters.
W_s	Container weight capacity of section s in tons.
V_s	Container volume capacity of section s in TEU.
R_s	Number of reefer plugs in section s.
Φ_s, Ψ_s, Θ_s	Buoyancy linearisation constants of section s.
W_τ	Weight of container type τ in tons.
V_τ	Volume of container type τ in TEU.
R_τ	Indicates whether container type τ is reefer.
d	Draft aft in meters at the stern of the vessel.
tr	Trim of the vessel in meters.
w_s	Weight of section s in tons.
b_s	Buoyancy of section s in tons.
r_s	Resulting force acting on section s in tons.
sf_s	Shear force between section $s-1$ and s in tons.
bm_s	Bending moment between section $s-1$ and s in tons meters.
t_s	Weight of tank content of section s in tons.
c_s^τ	Number of containers of type τ in section s.

Table 1. Sets, constants, and variables used in the SCM.

complete physical partitioning of the vessel such that all of its parts belong to a section and no part belongs to two sections. Section borders are aligned with bays, and a section cannot divide a bay. An example of a section partitioning with six sections is shown with green boxes in Fig 1. Let $L_s^G = \frac{L_s}{2} + \sum_{s'>s} L_{s'}$ denote the distance from the stern to the center of gravity (mid-point) of section s. Further, let $L_s^F = \sum_{s' \geq s} L_{s'}$ denote the distance to the fore boundary of section s (reference point for stress forces). A container type $\tau \in \mathcal{T}$ is a triple (l, r, w), where $l \in \{20, 40, 45\}$ is the length of the container, $r \in \{RF, NR\}$ is the reefer property of the container (reefer or non-reefer), $w \in \{9, 14, 29\}$ is the weight class of the container expressed as the average weight of containers in the class in metric tons. The buoyancy linearisation constants Φ_s,Ψ_s, and Θ_s of section s are approximated using (1). The domain of all variables is $\mathbb{R}_0^+$. In particular, this means that we relax the integrality of c_s^τ. Previous work shows negligible impact of this relaxation in practice [10], due to the large number containers in each bay (near 1000 on average on modern vessels). Also notice that none of the variables are identified as decision variables. This is on purpose since any subset of the variables can act as decision variables depending on the application of the SCM.

The SCM is a polyhedron over the variables defined by the following linear equations and inequalities.

$$b_s = \Phi_s d + \Psi_s tr + \Theta_s \qquad \forall s \in \mathcal{S} \tag{2}$$

$$w_s = W_s^0 + t_s + \sum_{\tau \in \mathcal{T}} W_\tau c_s^\tau \qquad \forall s \in \mathcal{S} \tag{3}$$

$$r_s = b_s - w_s \qquad \forall s \in \mathcal{S} \tag{4}$$

$$\sum_{s \in \mathcal{S}} w_s = \sum_{s \in \mathcal{S}} b_s \qquad \sum_{s \in \mathcal{S}} L_s^G r_s = 0 \tag{5}$$

$$sf_s = \sum_{s' < s} r_{s'} \qquad \forall s \in \mathcal{S} \setminus \{1\} \tag{6}$$

$$bm_s = \sum_{s' < s} (L_{s'}^G - L_s^F) r_{s'} \qquad \forall s \in \mathcal{S} \setminus \{1\} \tag{7}$$

$$\mathrm{SF}_s^- \leq sf_s \leq \mathrm{SF}_s^+ \qquad \forall s \in \mathcal{S} \setminus \{1\} \tag{8}$$

$$\mathrm{BM}_s^- \leq bm_s \leq \mathrm{BM}_s^+ \qquad \forall s \in \mathcal{S} \setminus \{1\} \tag{9}$$

$$\sum_{\tau \in \mathcal{T}} W_\tau c_s^\tau \leq W_s \qquad \forall s \in \mathcal{S} \tag{10}$$

$$\sum_{\tau \in \mathcal{T}} V_\tau c_s^\tau \leq V_s \qquad \forall s \in \mathcal{S} \tag{11}$$

$$\sum_{\tau \in \mathcal{T}} R_\tau c_s^\tau \leq R_s \qquad \forall s \in \mathcal{S} \tag{12}$$

Equation (2) defines the buoyancy of section s as a linear expression over aft draft d and trim tr. The linearisation coefficients Φ_s and Ψ_s and constant Θ_s are estimated from the linearisation of the Bonjean curves using equation (1) to calculate buoyancy of a section. Equation (3) defines the weight of section s as the sum of the lightship fraction within the section, the weight of fluids in tanks of the section, and the weight of cargo stowed in the section. Equation (4) defines the resulting vertical force r_s acting on section s. Since the positive direction is upward, buoyancy counts positive, while gravity counts negative. The two equalities of Equation (5) ensure that the vessel is in hydrostatic equilibrium. The first equation says that at hydrostatic equilibrium, the total buoyancy of the hull must equal the total weight of the vessel. Otherwise, it must go to a higher or lower draft to be in equilibrium. Also at hydrostatic equilibrium, the sum of longitudinal moments of any cross-section must be zero. Otherwise, the vessel must go to a higher or lower trim to be in equilibrium. The second equation expresses the constraint for the cross-section at origo (the stern). Equation (6) defines the shear force at the fore boundary of section s. Since the shear force is the sum of resulting forces acting fore of this cross-section, we add the resulting forces of all sections in front of the point. Notice that we do not compute shear force at the fore boundary of the first section. This boundary is at the very tip of the vessel, where the shear force by definition is zero. Equation (7) defines the bending moment at the fore boundary of section s. We now have to multiply

the resulting force with the distance $L_s^G - L_s^F$ to it. Again, we do not compute bending moment for the fore boundary of the first section, since it is zero. The limits of shear force and bending moment are ensured by Equation (8) and (9). The last three inequalities are stowage capacity constraints. Equation (10)-(12) ensure that the weight, volume, and reefer requirements of containers stowed in a section are within the capacity of the section. As shown in industrial projects [9], these constraints can be extended with advanced linear trade-offs between container types and weight classes. We plan to integrate these constraints into the SCM in future work.

4 Experimental Results

The purpose of the experiments is to evaluate the hydrostatic core of the SCM introduced in this paper. Specifically, we investigate the accuracy of the model's hydrostatic parameters as a function of given weight distributions, as well as the accuracy of the model in terms of the number of sections in the section partitioning.

The experiments are based on the 15000 TEU vessel introduced in the last section. For this vessel, we have access to the hydrostatic table approved by its classification society. For a given lcg and displacement, we can use this table to find the associated trim and draft at hydrostatic equilibrium and compare with the values predicted by the SCM. The table, however, does not include the stress forces over the vessel. To find these, we construct a vessel condition corresponding to the equilibrium and use an approved loading computer of the vessel [6] to calculate the forces that we then compare to the ones predicted by the SCM.

We have chosen three different weight levels at 100%, 80%, and 60% of maximum summer displacement. Notice that since about 35% of the weight of the vessel is steel and fuel, the vessel is usually less than half full by volume of cargo at 60% of maximum displacement. For each of the three displacement levels, we use 10 different cargo weight distributions over its bays corresponding to an operational lcg range. Water ballast tanks are assumed to be empty, while all other tanks are assumed to be 70% full by volume.[3]

The real hydrostatic equilibrium of the vessel has been approximated as follows. We first compute the displacement and lcg of the vessel using the longitudinal positions of lightship blocks, tanks, and bays stowed with one of the cargo weight distributions. Since these parameters decide the hydrostatic equilibrium of the vessel in the longitudinal dimension, we can lookup the associated draft and trim in the hydrostatic table. [4]

The equations of the SCM model have been implemented in Java and solved with the JAMA matrix package for given weight distributions. The CPU time

[3] These constant weight blocks of tanks are added to the lightship blocks in these experiments.

[4] Due to the sparsity of the hydrostatic table, in practice we interpolate the trim and draft from nearby entries.

required for these computations is negligible (less than one second in all cases). From these computations, we get the trim, draft (adjusted from aft to mid-ship draft), and stress forces predicted by the SCM. Lcg is non-linear in the SCM variables and therefore not included in the model. For a given cargo weight distribution, however, we can compute the underlying lcg of the SCM, since it assumes that all weights of a section s act from their approximated center of gravity, L_s^G.

4.1 Variable Displacement, Fixed Number of Sections

In the first set of experiments, we use the most detailed version of the SCM, where each section at most holds a single bay. This model has 26 sections. Table 2 shows the trim, draft, and lcg predicted by the SCM for 100%, 80%, and 60% of maximum displacement. The draft predictions are quite accurate. The

	Real Values			SCM Values		
Disp. (ton)	Trim (m)	Draft (m)	Lcg (m)	Trim (m)	Draft (m)	Lcg (m)
218788	2.01	15.6	-14.9	4.19	16.0	-14.9
(100%)	1.61	15.6	-14.1	3.55	16.0	-14.2
	1.20	15.6	-13.3	2.90	16.0	-13.4
	0.80	15.7	-12.6	2.26	16.0	-12.6
	0.40	15.7	-11.8	1.63	16.0	-11.9
	0.00	15.7	-11.0	0.99	16.1	-11.1
	-0.41	15.7	-10.3	0.36	16.1	-10.3
	-0.80	15.8	-9.5	-0.26	16.1	-9.6
	-1.21	15.8	-8.8	-0.88	16.1	-8.8
	-1.61	15.8	-8.0	-1.50	16.1	-8.1
175030	2.01	13.1	-13.0	2.35	13.1	-13.1
(80%)	1.61	13.1	-12.2	1.82	13.1	-12.3
	1.20	13.1	-11.4	1.27	13.1	-11.4
	0.80	13.2	-10.6	0.73	13.1	-10.6
	0.39	13.2	-9.8	0.20	13.1	-9.8
	0.00	13.2	-9.0	-0.32	13.2	-9.0
	-0.40	13.2	-8.3	-0.82	13.2	-8.3
	-0.80	13.2	-7.5	-1.34	13.2	-7.5
	-1.21	13.2	-6.7	-1.85	13.2	-6.7
	-1.61	13.3	-6.0	-2.35	13.2	-6.0
131272	2.02	10.4	-12.3	1.71	10.2	-12.3
(60%)	1.61	10.4	-11.4	1.25	10.2	-11.4
	1.21	10.4	-10.5	0.80	10.2	-10.5
	0.80	10.4	-9.6	0.36	10.2	-9.6
	0.41	10.5	-8.7	-0.07	10.2	-8.8
	0.00	10.5	-7.8	-0.53	10.2	-7.8
	-0.39	10.5	-7.0	-0.96	10.2	-7.0
	-0.80	10.5	-6.1	-1.39	10.2	-6.1
	-1.21	10.5	-5.2	-1.84	10.3	-5.2
	-1.60	10.5	-4.4	-2.25	10.3	-4.4

Table 2. Trim, draft, and lcg predicted by the SCM for 100%, 80%, and 60% of maximum displacement using a partitioning with 26 sections.

highest deviation is about 40 centimeters and only seen at 100% of maximum displacement.

The correlations between the real trim and lcg and the predicted trim and lcg are shown in Fig. 5. As depicted in Fig. 5(c), the lcg prediction of the SCM is

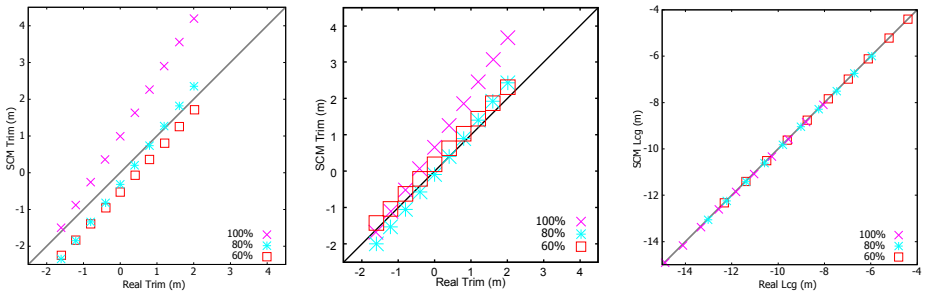

Fig. 5. (a-b) Correlation between real and predicted trim for two linearisation choices of the Bonjean curves. (c) Correlation between real and predicted lcg. In each case, a fixed partitioning with 26 sections and 60%, 80%, and 100% of maximum displacement were used.

highly accurate for all weight distributions. This is not a trivial result. We have that the longitudinal position of cargo weight is at the center of sections independently of the number of sections. This, however, is not the case for lightship and tank blocks that usually are misaligned with section boundaries. What the results show is that impact on lcg at this level of detail is negligible.

An accurate lcg prediction is needed for an accurate trim prediction of the SCM. The trim prediction, however, also includes error caused by the buoyancy approximation. The SCM trim predictions shown in Fig. 5(a) uses the linearisation of Bonjean curves partly shown in Fig. 3(c,d). The trim predictions are very accurate for 80% and 60% of maximum displacement. Keep in mind that the vessel is almost 400 meters long, so the differences of about 30 centimeters is an angular error of less than 0.1%. We attribute the higher error at 100% of maximum displacement to the underestimate of the buoyancy of the stern. To test this hypothesis, we changed the linearisation to best fit within a displacement range corresponding to between 60% and 100% maximum displacement. Since this range starts at about 10 meters draft, the linearisation of the stern curves become more accurate (e.g., see Fig. 3(c)). The resulting trim prediction is shown in Fig. 5(b) and shows significant accuracy improvement as expected.

4.2 Variable Number of Sections, Fixed Displacement

In the second set of experiments, we fix the displacement to 80% of maximum, while the numbers of sections vary from 26 to 4. The trim and lcg predictions are shown in Table 3 and 4, respectively. The correlations between the real trim and

Real Values			SCM Trim for 26 to 4 Sections					
Trim (m)	Draft (m)	Lcg (m)	26	13	10	8	6	4
2.01	13.11	-13.02	2.35	2.40	2.54	1.65	0.78	0.39
1.61	13.13	-12.21	1.82	1.86	2.02	1.12	0.24	-0.16
1.20	13.15	-11.38	1.27	1.31	1.47	0.57	-0.30	-0.68
0.80	13.16	-10.58	0.73	0.79	0.95	0.00	-0.88	-1.20
0.39	13.18	-9.79	0.20	0.26	0.42	-0.50	-1.37	-1.71
0.00	**13.20**	**-9.01**	**-0.32**	**-0.26**	**-0.11**	**-1.01**	**-1.87**	**-2.22**
-0.40	13.21	-8.25	-0.82	-0.76	-0.61	-1.54	-2.40	-2.72
-0.80	13.23	-7.47	-1.34	-1.28	-1.12	-2.03	-2.93	-3.20
-1.21	13.25	-6.71	-1.85	-1.79	-1.66	-2.57	-3.44	-3.79
-1.61	13.26	-5.96	-2.35	-2.29	-2.14	-3.08	-3.94	-4.29

Table 3. Trim predicted by the SCM for 80% of maximum displacement using six different partitionings.

Real Values			SCM Lcg for 26 to 4 Sections					
Trim (m)	Draft (m)	Lcg (m)	26	13	10	8	6	4
2.01	13.11	-13.02	-13.06	-13.12	-13.21	-11.88	-11.14	-11.09
1.61	13.13	-12.21	-12.25	-12.33	-12.42	-11.09	-10.31	-10.23
1.20	13.15	-11.38	-11.42	-11.49	-11.61	-10.27	-9.48	-9.43
0.80	13.16	-10.58	-10.62	-10.72	-10.84	-9.43	-8.59	-8.63
0.39	13.18	-9.79	-9.82	-9.91	-10.05	-8.68	-7.84	-7.85
0.00	**13.20**	**-9.01**	**-9.04**	**-9.13**	**-9.26**	**-7.92**	**-7.08**	**-7.06**
-0.40	13.21	-8.25	-8.29	-8.38	-8.51	-7.13	-6.28	-6.28
-0.80	13.23	-7.47	-7.51	-7.60	-7.76	-6.41	-5.46	-5.54
-1.21	13.25	-6.71	-6.74	-6.83	-6.95	-5.60	-4.69	-4.64
-1.61	13.26	-5.96	-6.00	-6.09	-6.23	-4.84	-3.92	-3.86

Table 4. Lcg predicted by the SCM for 80% of maximum displacement using six different partitionings.

lcg and the predicted trim and lcg for these experiments are shown in Fig. 6(a) and (b), respectively. As depicted Fig. 6(b), the lcg positions predicted by the SCM are systematically off for the coarser partitionings with 8, 6, and 4 sections with a fixed amount. This error may be due to the misalignment of lightship blocks and tanks which will be more significant at courser levels of the model. The trim results shown in Fig. 6(a) are off correspondingly. Since each section partitioning forms an independent SCM model, it should be possible to reduce its trim error (and related stress force error) by adjusting the fixed position of the longitudinal center of gravity of its sections.

4.3 Stress Forces

In order to evaluate the stress forces predicted by the SCM, we construct a condition of the vessel at 80% of maximum summer displacement in an approved loading computer [6] corresponding to row six (bold) of Table 3 and 4. The real trim of this condition is zero and the SCM predicts it to be -0.32 meters. Despite this buoyancy inaccuracy of the SCM, the stress force predictions are remarkably accurate even for coarse partitionings with 8 and 6 sections. The results are shown in Fig. 7. The solid curves are the real forces calculated by the loading computer. Notice that the shear force curve is uneven. This is expected given the lightship weight distribution of the vessel. A bending curve is usually

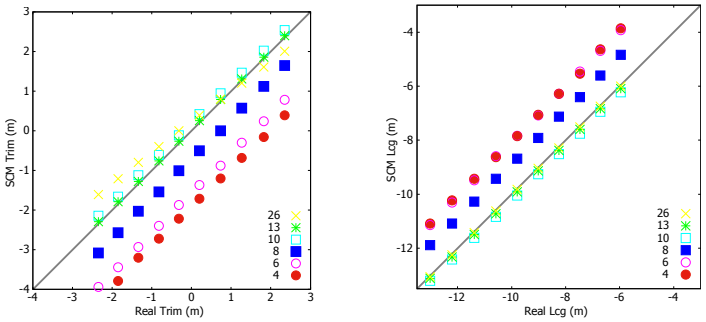

(a) (b)

Fig. 6. Correlations between real and predicted trim (a) and lcg (b) for a fixed 80% of maximum displacement and six different section partitionings.

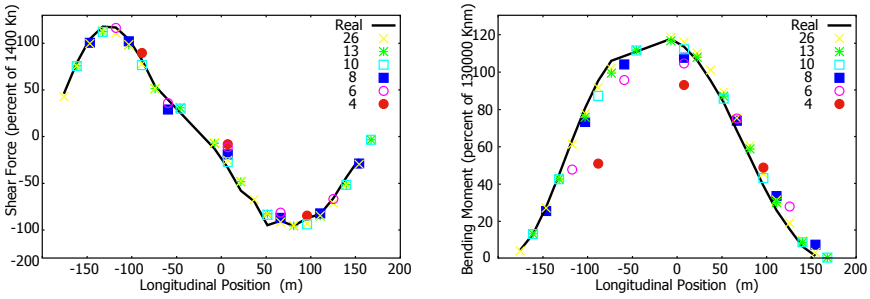

(a) (b)

Fig. 7. Shear force (a) and bending moment (b) predictions for a fixed 80% of maximum displacement and six different section partitionings.

smooth even for an uneven weight distribution. The impression of the curve at -50 meters lcg is due to a missing measure point over the accommodation of the vessel.

5 Conclusion and Future Work

In this paper, we have introduced the Standard Capacity Model (SCM). The objective of our work on the SCM is to provide a polyhedron representation of container vessel capacity that can be integrated in higher order optimization models like cargo flow networks for uptake and revenue management. Further, the aim is to enable the modelling of vessel capacity and key parameters substantially more accurate than is done today without sacrificing tractability. In this paper, we have introduced the hydrostatic core of the SCM, which to our knowl-

edge is the first polyhedron approximation to hydrostatic equilibria of container vessels that allow variable displacement.

Our results show that the box-shaped hull approximation of sections applied by the SCM is realistic in typical sailing conditions and leads to accurate draft, trim, and stress force predictions also for coarse section partitionings. The results are well within the precision needed for practical application in the liner shipping industry. In future work, we plan to extend the model with advanced linear trade-offs between container types and weight classes shown in industrial projects [9]. We also consider applying regression analysis to find the longitudinal center of gravity of each section with minimum trim error such that the systematic errors seen in Fig. 6 can be reduced. A similar approach can be used to make a linear approximation to the metacentric height (i.e., transversal stability) of the vessel.

References

1. Ambrosino, D., Paolucci, M., Sciomachen, A.: A MIP heuristic for multi poty stowage planning. Transportation Research Procedia **10**, 725–734 (2015)
2. Avriel, M., Penn, M., Shpirer, N.: Container ship stowage problem: complexity and connection to the coloring of circle graphs. Discrete Applied Mathematics **103**, 271–279 (2000)
3. Delgado, A.: Models and Algorithms for Container Vessel Stowage Optimization. Ph.D. thesis, IT University of Copenhagen (2013)
4. Economist: The humble hero (May 2013)
5. Economist: Thinking outside the box (April 2018)
6. Interschalt: MACS3 loading computer. http://navis.com
7. Kang, J., Kim, Y.: Stowage planning in maritime container transportation. Journal of the Operations Research Society **53**(4), 415–426 (2002)
8. Li, F., Tian, C., Cao, R., Ding, W.: An integer linear programming for container stowage problem. Lecture Notes in Computer Science, vol. 5101, pp. 853–862. Springer (2008)
9. Optivation: Mathematical cargomix optimization model for the K-class (2013)
10. Pacino, D., Delgado, A., Jensen, R., Bebbington, T.: Fast generation of near-optimal plans for eco-efficient stowage of large container vessels. Lecture Notes in Computer Science, vol. 6971, pp. 286–301. Springer (2011)
11. Pacino, D., Delgado, A., Jensen, R., Bebbington, T.: An Accurate Model for Seaworthy Container Vessel Stowage Planning with Ballast Tanks, pp. 17–32 (2012)
12. Parreo, F., Pacino, D., Alvarez-Valdes, R.: A GRASP algorithm for the container stowage slot planning problem. Transportation Research Part E: Logistics and Transportation Review **94**, 141 – 157 (2016)
13. Tierney, K., Pacino, D., Jensen, R.: On the complexity of container stowage planning problems. Discrete Applied Mathematics **169**, 225 – 230 (2014)
14. UNCTAD: Review of maritime transport 2016. United nations conference on trade and development UNCTAD (2016)
15. Wilson, I., Roach, P.: Principles of combinatorial optimization applied to container-ship stowage planning. Journal of Heuristics **5**, 403–418 (1999)
16. Zurheide, S., Fischer, K.: A revenue management slot allocation model for liner shipping networks. Maritime Economics & Logistics **14**(3), 334–361 (2012)